International Immunology, Vol. 32, No. 3, pp. 203–212
doi:10.1093/intimm/dxz070
Advance Access publication 20 October 2019

ZBP1 governs the inflammasome-independent IL-1α and neutrophil inflammation that play a dual role in anti-influenza virus immunity

Masatoshi Momota[1–3], Patrick Lelliott[4], Atsuko Kubo[1], Takato Kusakabe[1–3], Kouji Kobiyama[1,5,6], Etsushi Kuroda[1,3,7], Yumiko Imai[8], Shizuo Akira[9], Cevayir Coban[4,6,10] and **Ken. J. Ishii[1–3,5,6]**

[1]Laboratory of Adjuvant Innovation and
[2]Laboratory of Mockup Vaccine, Center for Vaccine and Adjuvant Research Center (CVAR), National Institutes of Biomedical Innovation, Health and Nutrition (NIBIOHN), Osaka 567-0085, Japan
[3]Laboratory of Vaccine Science and
[4]Malaria Immunology, World Premier International Immunology Frontier Research Center, Osaka University, Osaka 565-0871, Japan
[5]Division of Vaccine Science and
[6]International Research and Development Center for Mucosal Vaccines, The Institute of Medical Science, The University of Tokyo, Tokyo 108-0071, Japan
[7]Department of Immunology, Hyogo College of Medicine, Hyogo 663-8501, Japan
[8]Laboratory of Regulation of Intractable Infectious Diseases, Center for Vaccine and Adjuvant Research Center (CVAR), National Institutes of Biomedical Innovation, Health and Nutrition (NIBIOHN), Osaka 567-0085, Japan
[9]Host Defense, World Premier International Immunology Frontier Research Center, Osaka University, Osaka 565-0871, Japan
[10]Division of Malaria Immunology, The Institute of Medical Science, The University of Tokyo, Tokyo 108-0071, Japan

Correspondence to: K. J. Ishii; E-mail: kenishii@ims.u-tokyo.ac.jp

Received 4 September 2019, *editorial decision* 14 October 2019; *accepted* 17 October 2019

Abstract

Influenza A virus (IAV) triggers the infected lung to produce IL-1 and recruit neutrophils. Unlike IL-1β, however, little is known about IL-1α in terms of its mechanism of induction, action and physiological relevance to the host immunity against IAV infection. In particular, whether Z-DNA-binding protein 1 (ZBP1), a key molecule for IAV-induced cell death, is involved in the IL-1α induction, neutrophil infiltration and the physiological outcome has not been elucidated. Here, we show in a murine model that the IAV-induced IL-1α is mediated solely by ZBP1, in an NLRP3-inflammasome-independent manner, and is required for the optimal IL-1β production followed by the formation of neutrophil extracellular traps (NETs). During IAV infection, ZBP1 displays a dual role in anti-IAV immune responses mediated by neutrophils, resulting in either protective or pathological outcomes *in vivo*. Thus, ZBP1-mediated IL-1α production is the key initial step of IAV-infected NETs, regulating the duality of the consequent lung inflammation.

Keywords: IL-1, influenza virus, innate immunity, neutrophil, ZBP1

Introduction

High morbidity and mortality following lethal influenza A virus (IAV) infection are well correlated with the lung epithelial cell damage, which is caused by excessive inflammatory cell infiltration and robust host immune activation (1–3). This is reflected in systemic analyses of IAV-infected mice, where the infiltrating neutrophils and/or macrophages are the major drivers into the inflammatory cycle culminating in irreversible, severe lung damage and acute death due to IAV infection (4). Indeed, blockage of immune cell migration causes reduced cytokine production during the acute phase of IAV infection, independently of systemic immune activation and viral replication (5). The local secretion of cytokines such as IL-1 is nevertheless indispensable for viral control and host survival demonstrated by IAV infection in IL-1 receptor (IL-1R)-deficient mice (6). Consistent with this observation, subsequent studies revealed that the NLRP3 inflammasome is essential for IL-1β maturation and secretion and subsequent protection against IAV infection (7–9).

IL-1α, an alternative agonist for IL-1R in addition to IL-1β, has been described as a unique nuclear cytokine which is responsible for the priming of inflammatory responses in not only sterile conditions but also microbial infections (10–13). Unlike

IL-1β, pro-IL-1α is constitutively expressed in various types of cells in the tissue and does not require enzymatic cleavage for maturation, where the membrane rupture through necrotic or necroptotic cell death is sufficient for the secretion of an active form of IL-1α, without a requirement for protein synthesis and caspase-1/11 activation (14–17). Consistent with these reports, a recent study revealed that kinase receptor-interacting protein 3 (RIP3)-dependent necroptotic cell death is tightly correlated with IL-1α and β secretion and inflammatory responses (18). Furthermore, in IAV infection, RIP3 and its upstream factor Z-DNA-binding protein 1 (ZBP1) were shown to control not only necroptotic cell death (19–21) but also NLRP3 activation and IL-1β secretion (22).

In spite of accumulating evidence, little is known about IL-1α. More specifically, the roles of NLRP3 inflammasome activation and ZBP1-mediated cell death in the IAV-induced IL-1α production as well as their physiological relevance to IAV infection and immunity have not been clarified. In particular, whether ZBP1 plays a protective or pathological role during the immunity to IAV infection has been controversial (20, 21). Therefore, in this study, we examined whether ZBP1 is involved in IAV-induced IL-1α secretion and consequent inflammatory responses in IAV-infected mouse lung, that lead to either protective or pathological immune responses.

Methods

Mice and cells

C57/BL6 mice and those in the same genetic background, except *Zbp1*$^{+/-}$ and *Zbp1*$^{-/-}$, *Il1r1*$^{+/-}$, *Il1r1*$^{-/-}$, *Il1a*$^{+/-}$, *Il1a*$^{-/-}$, *Nlrp3*$^{+/-}$, *Nlrp3*$^{-/-}$, *Asc*$^{+/-}$, *Asc*$^{-/-}$, *Caspase-1/11*$^{+/-}$ and *Caspase-1/11*$^{-/-}$, were housed in a specific pathogen free environment for 7–10 weeks. All experiments were carried out according to the protocol approved by the animal experiment committee for the National Institute of Biochemical Innovation, Health and Nutrition (DS22-34, DS24-56). Primary bone marrow-derived macrophages (BMDMs), alveolar macrophages and lung primary fibroblasts were generated as previously described (23). For lipopolysaccharide (LPS) priming, BMDMs were incubated with 100 ng ml^{-1} of LPS for 4 h, and then the medium was removed and the cells were washed with phosphate-buffered saline (PBS) twice before the IAV infection. For virus preparation and plaque assays, MDCK cells were obtained from the JCRB cell bank (JCRB9029, National Institute of Biomedical innovation, Health and Nutrition, Japan) and maintained accordingly.

Antibodies

Antibodies for flow cytometry staining were obtained from the following sources as 'Fluorescence color-antigen (clone name)': FITC-CD45 (30-F11), PerCP/Cy5.5-CD11b (M1/70), BV421-Ly6G (1A8), PerCP/Cy5.5-CD3ε (145-2C11), PE-Cy7 anti-Ly6G (1A8), BV570-CD8α (53-6.7), APC-TCR-b (H57-597) and BV421-CD62L (MEL-14) from Biolegend, Cy5PE-CD44 (1M7) from BD Bioscience, and LIVE/DEAD™ Fixable Blue Dead Cell Stain Kit and SYTOX green were from Thermo Fisher Scientific, Hoechst 33342 was from Sigma-Aldrich and H-2D^{b} Influenza NP Tetramer-ASNENMETM-PE was from MBL. FITC-Ly6G (1A8) antibody (Biolegend) and Hoechst 33342 (DOJINDO) were used in 2-photon imaging microscopy. LPS (Sigma-Aldrich), z-VAD(OMe)-FMK (Cayman Chemical), Necrostatine-1 (Focus Biomolecules) and GSK'872 (BioVision) were used for *in vitro* BMDM experiments. .

In vitro infection and measurement of cytokine and cell death

BMDMs (2 × 10^{5}) were stimulated with live virus, inactivated virus or the other stimuli. IAV was inactivated by exposure to 12 000 J of UV light with stratalinker 1800 (Stratagene, USA). Whole IAV genomic RNA was extracted from live IAV by TRIZOL-LS reagents (Thermo Fisher Scientific) and 1 μg ml^{-1} of IAV genomic RNA was transfected to BMDMs with lipofectamine 2000 (Thermo Fisher Scientific). After each stimulation, the concentrations of IL-1α (Bio Legend), IL-1β (R&D Systems) or IFNβ (PBL) were measured by ELISA according to the manufacturer's protocols. To quantitate the cell death *in vitro*, lactate dehydrogenase (LDH) release in the supernatants of the cell culture was measured by cytotoxicity detection kit LDH (Roche Diagnostic).

Virus, infection and adaptive immune response

Virus preparation and infections were performed as previously described (24). In brief, IAV (A/Puerto Rico/8/34 strains) was propagated in MDCK cells. All viruses were titrated by agar overlay plaque assay in propagated cells. For *in vivo* experiments, sex- and age-matched mice were anesthetized with intra-peritoneal injection of ketamine (80 mg kg^{-1}) and xylazine (8 mg kg^{-1}) and infected intra-nasally with 50 pfu of IAV (1LD$_{50}$ dose) in 30 μl of PBS, or intra-tracheally with the same dose of virus in 50 μl of PBS. To analyze the survival rate, weight loss of infected mice was monitored daily for 21 days. For broncho-alveolar lavage fluid (BALF) and lung histology analysis, mice were euthanized by overdose of anesthetic reagents at indicated time points. To relate to a human endpoint, >35% body weight loss was considered as moribund and mice were euthanized accordingly. Seven days after infection, PR8 influenza HA-specific IgG, IgA, IgM, IgG1 and IgG2c titers in the serum and BALF were determined by ELISA using a split-product of influenza PR8 hemagglutinin (The Research Foundation for Microbial Diseases of Osaka University, Japan) coated plate and horseradish peroxidase-conjugated anti-mouse immunoglobulin antibodies as described previously (25). Numbers of NP-specific tetramer positive CD8 T cells in the spleen, lung regional lymph nodes, BALF and the lung homogenates were determined by PE-conjugated tetramer staining within CD3-, TCR-β-, CD8-, CD44- and CD62L-positive cells.

Cellular and histological analysis of infected BALF and lung tissue

BALF was collected by washing the trachea and lungs from the infected mice twice with 600 μl of ice cold PBS. Cell-free BALF was analyzed for concentrations of IL-1α or IL-1β by ELISA, for double-strand DNA release by Nano-drop (Thermo Fisher Scientific, USA), and for virus titration by plaque assay using MDCK cells. BAL cells were stained with anti-CD16/CD32, LIVE/DEAD™ Fixable Blue Dead Cell Stain

Kit, anti-CD45, anti-CD11b and anti-Ly6G. After staining, cells were washed twice with PBS and then fixed with 1% paraformaldehyde in PBS solution. Samples were collected by a LSRII flow cytometer (BD Biosciences, USA), and neutrophils in BALF were gated and analyzed based on Ly6G- and CD11b-positive cells within live CD45-positive leukocyte cells by FlowJo software (Tree Star). For H&E staining, the lung was inflated with Mildform 10 N reagent injection via the intra-tracheal route, and was removed and fixed in Mildform reagent for 12 h. Paraffin-embedded lung samples were sliced and stained using a standard H&E protocol.

Neutrophil depletion

For *in vivo* neutrophil depletion, 200 μg of anti-mouse Ly6G (1A8) or control IgG2a (2A3) (Biolegend) was injected intraperitoneally. Antibody treatment was started at 24 h before infection and followed each 48 h for three times until day 5 post-infection.

Two-photon microscope and imaging flow cytometry

On day 3 after IAV infection, mice were killed by an overdose of ketamine and xylazine. For 2-photon microscope analysis, anti-Ly6G antibody and Hoechst 33342 were injected into the lungs of mice intra-tracheally. Fifteen minutes after injection, the lung was cut coronally and observed by FV1000MPE2 (Olympus, Japan). Image stream analysis of neutrophil extracellular traps (NETs) was performed as described previously (26). Briefly, BALF collected from IAV-infected mice was stained with 1 μg ml^{-1} PE-Cy7 anti-Ly6G antibody, 25 nM SYTOX Green and 1.6 μM Hoechst for 30 min at room temperature. Neutrophils and NETs were analyzed with an ImageStream X Mark II imaging flow cytometer (Millipore, USA) using the 60× objective at low flow and high sensitivity with 'retain clipped images' turned on. Laser power was set to 120 and 200 mW for the 405 and 488 nM lasers, respectively. Events with a brightfield area greater than 20 μm^2 or a SYTOX green area greater than 20 μm^2 were collected for analysis. Masking was performed using the 'object' and 'morphology' algorithm, with the 'extracellular DNA area' feature calculated by subtracting the brightfield 'object' mask from the SYTOX Green 'morphology' mask. IDEAS v6.2 and Flowjo V10 was used for analysis.

Statistical analysis

Statistical analyses between data sets were performed using two-tailed Student's *t*-test. Survival data were analyzed with a log-rank Mantel–Cox test. All statistical analysis was performed using Prism Graph Pad analysis (GraphPaD, version 7.04).

Results and discussion

IL-1α is required for the optimal IL-1β production and host defense against IAV infection

The importance of IL-1 in protective immune responses to IAV infection has been demonstrated by studies in which IL-1β deficiency, or inhibition of IL-1 signaling by IL-1R antagonist, displayed increased susceptibility to IAV infection (27, 28). Indeed, IL-1R-deficient mice display reduced acute pulmonary inflammatory responses, followed by an impaired acquired immune response resulting in the reduced survival (6, 29). Although these studies had revealed an importance of IL-1β and IL-1R signaling, the potential role of IL-1α has not been clarified, or overlooked otherwise. To uncover the specific role of IL-1α in IAV infection, we infected *Il1a*$^{+/-}$ and *Il1a*$^{-/-}$ mice with a sub-lethal dose of IAV (H1N1 A/PR/8/34 strain, 50 pfu per head = 1 LD_{50}). *Il1a*$^{-/-}$ mice infected with IAV suffered from significantly increased mortality compared with *Il1a*$^{+/-}$ mice, at a similar degree observed between *Il1r1*$^{+/-}$ and *Il1r1*$^{-/-}$ mice (Fig. 1A and B). We then measured the IL-1β concentration in the BALF of the infected mice on day 3, and found that BALF IL-1β was significantly reduced not only in *Il1r1*$^{-/-}$ but also in *Il1a*$^{-/-}$ mice (Fig. 1C). In contrast, IL-1α levels in the same BALF were not altered in *Il1r1*$^{-/-}$ mice BALF (Fig. 1D). These data suggest that IL-1α is required for the host protection against lethal infection with IAV, and for the optimal IL-1β production *in vivo* after IAV infection that requires IL-1R. Thus, IL-1α is induced upon IAV infection and acts upstream of the IL-1R-mediated optimal production of IL-1β, while it has been known that IL-1α can form a positive feedback loop for IL-1β induction during inflammation (30–32). Of note, both *Il1a*$^{-/-}$ mice and *Il1r1*$^{-/-}$ mice showed decreased pulmonary damage on day 3 compared with their control mice (Fig. 1E), but this resulted in the delayed clearance of IAV during later phases of infection and exfoliation of bronchiolar epithelial cells (Supplementary Figure S1A). Together these data confirmed the hierarchy between IL-1α and IL-1β, in which IL-1α is required for the optimal production of, and acts upstream of, IL-1β induced during the acute phase of IAV infection.

IAV-induced IL-1α secretion occurs independently of NLRP3, ASC and caspase-1/11

The NLRP3 inflammasome has been shown to be critical for IL-1β maturation and production and plays a reciprocal role in either protection or pathogenesis during IAV infection through IL-1 receptor signaling (7, 29, 33, 34); however, whether the NLRP3 inflammasome is involved in IL-1α induction during IAV infection remains unknown. To address this issue, we infected mice lacking components of the inflammasome pathway, NLRP3, apoptosis-associated speck-like protein containing a CARD (ASC), or caspase-1/11, with a sub-lethal dose of IAV. In our experimental setting, not only did we find no differences in survival during infection in those inflammasome-deficient mice (Fig. 2A), but also we detected no changes in the levels of IL-1α in BALF (Fig. 2B). Furthermore, unlike previous studies, BALF IL-1β concentrations on day 3 were comparable among those inflammasome-deficient mice in our experimental setting (Fig. 2B). These discrepancies can arguably be explained to be due to differences of the infected IAV dose, the subclades, host resident microbiome, virome in the lung, gut, nasal, oral and even other organs, and potentially other factors such host metabolic status to body temperature to room temperature. Previous studies applied the exclusively high-dose infection model (1×10^3–6×10^4 PFU per dose) for detecting the NLRP3 inflammasome-dependent IL-1β secretion in BALF (7–9). In contrast, studies using a sub-lethal infection dose like ours (10–100 pfu or 0.4–1 LD_{50}) reported that NLRP3 has less of an effect on the host protection, in line

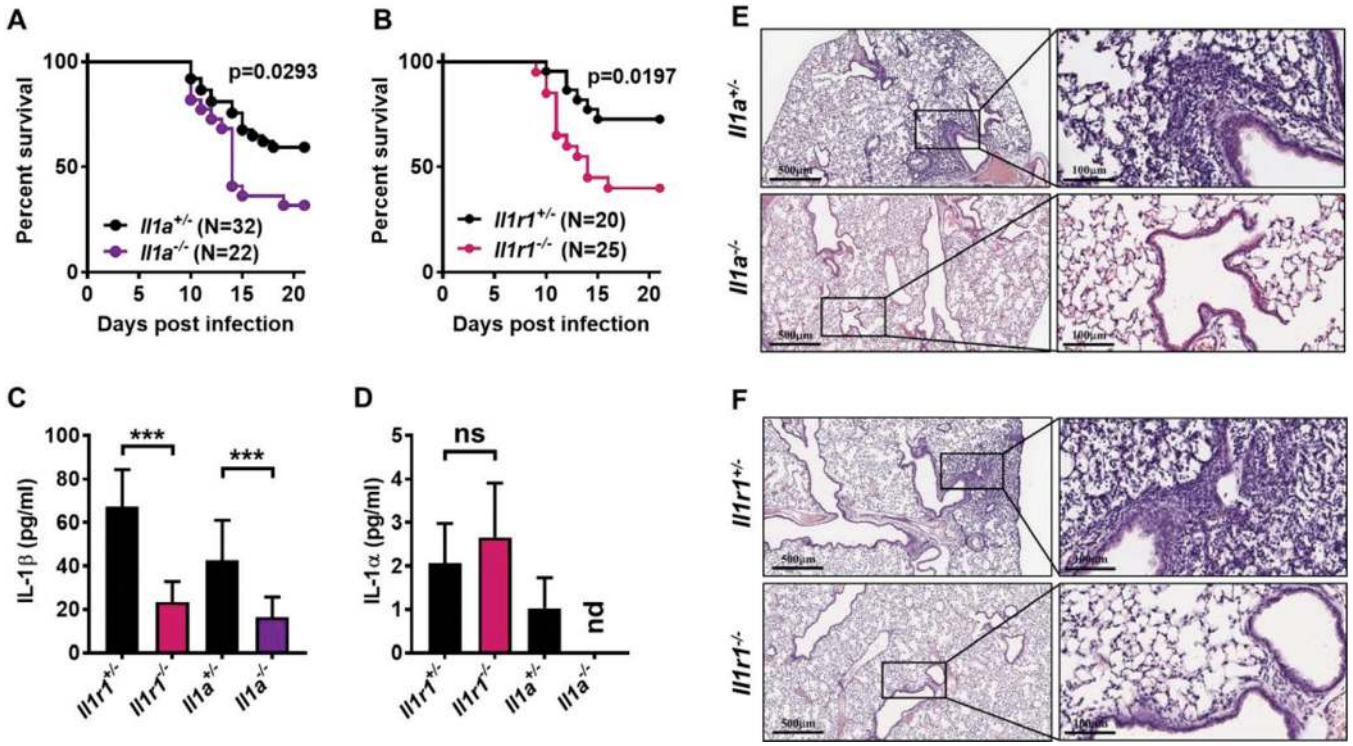

Fig. 1. IL-1α is required for the optimal IL-1β production and protection against sub-lethal IAV infection. Sex- and age-matched mice were infected with 1 LD_{50} of IAV via the intra-nasal route (A, B). Percentages of survived mice against IAV infection are shown for *Il1r1*- and *Il1a*-deficient mice (*N*: numbers of the analyzed mice) (C). IL-1β or (D) IL-1α concentrations of BALF from *Il1r1*$^{+/-}$, *Il1r1*$^{-/-}$, *Il1a*$^{+/-}$ or *Il1a*$^{-/-}$ mice on day 3 after IAV infection were measured by ELISA (N = 10–12 per group) (E and F). The lung tissues stained by H&E are shown for the *Il1r1*$^{+/-}$, *Il1r1*$^{-/-}$, *Il1a*$^{+/-}$ or *Il1a*$^{-/-}$ mice on day 3 after IAV infection. Statistical significances between each survival curve for the mice were determined by log-rank (Mantel–Cox) test (A and B). Error bars represent mean ± SD. ns, not significant; nd, not detected. ***P < 0.001.

with our results (6, 7, 35). Our findings above indicate a key role of inflammasome-independent IL-1α in the host protective responses against IAV infection at a low dose in particular, which may be reflected more in the natural infection.

IAV-induced IL-1α secretion is mediated solely by ZBP1 that coincides with cell death

To further clarify the mechanism(s) by which IAV induces IL-1α secretion *in vitro*, BMDMs derived from *Nlrp3*$^{-/-}$, *Asc*$^{-/-}$ or *Caspase-1/11*$^{-/-}$ mice were infected with IAV and their IL-1α secretion in the supernatant was measured by ELISA. Consistent with the data obtained *in vivo* (Fig. 2B), *Nlrp3*$^{-/-}$- and *Asc*$^{-/-}$-BMDM induced IL-1α at equivalent levels as their control *Nlrp3*$^{+/-}$ and *Asc*$^{+/-}$-BMDM cells, respectively (Fig. 2C and D). On the other hand, *Caspase-1/11*$^{-/-}$ cells showed significantly lower IL-1α secretion (P < 0.05; Fig. 2E). This indicates that IL-1α secretion is NLRP3 inflammasome-independent but partially dependent on Caspase-1/11, although their survival data *in vivo* showed its redundancy with other potential mechanism(s) (Fig. 2A).

IL-1α is a nuclear cytokine secreted from cells in a variety of mechanisms by which cellular stress, damage and death are triggered (15, 36). We previously reported that dying alveolar macrophages, but not lung fibroblasts, are a primary source of IL-1α that plays a crucial role for priming of inflammatory responses in the lung (23). Furthermore, recent studies have identified ZBP1 as a key molecule in IAV-induced cell death and IL-1β production (20–22). Consistent with these previous findings, IAV infection caused cell death measured by LDH release in around 30% of BMDM, 20% of alveolar macrophages and 10% of lung primary fibroblasts in a ZBP1-dependent manner (Fig. 2F; Supplementary Figure S1B).

By sharp contrast to the previous reports, however, the cell death induced by IAV was independent of NLRP3, ASC and caspase-1/11 (Fig. 2F). Similarly, IAV-induced IL-1β secretion in the same supernatants was significantly reduced in *Zbp1*$^{-/-}$ BMDM cells, but not in the *Nlrp3*$^{-/-}$, *Asc*$^{-/-}$ or *Caspase-1/11*$^{-/-}$ BMDM cells (Fig. 2G), whereas LPS-primed BMDM cells exhibited both ZBP1- and NLRP3/inflammasome-dependent IL-1β secretion with IAV infection (Fig. 2H), the latter of which was consistent with the previous report (22). We also reproduced the previous results that ZBP1-depdendent cell death required intact replication of the virus as UV-irradiated virus did not cause cell death (Supplementary Figure S1D), while transfection of viral RNA caused severe cell death, which was independent of ZBP1 (Supplementary Figure S1D), and that ZBP1-dependent cell death was inhibited by both pan-caspase and RIP3 inhibitor treatment (Supplementary Figure S1E), while ZBP1 deficiency had no direct effect on IAV replication and type-I IFN induction (Supplementary Figure S1F and G) (20, 22, 37).

Together with decreased cell death, not only the IAV-infected *Zbp1*$^{-/-}$ cells (Fig. 2I) but also BALF from *Zbp1*$^{-/-}$ mice

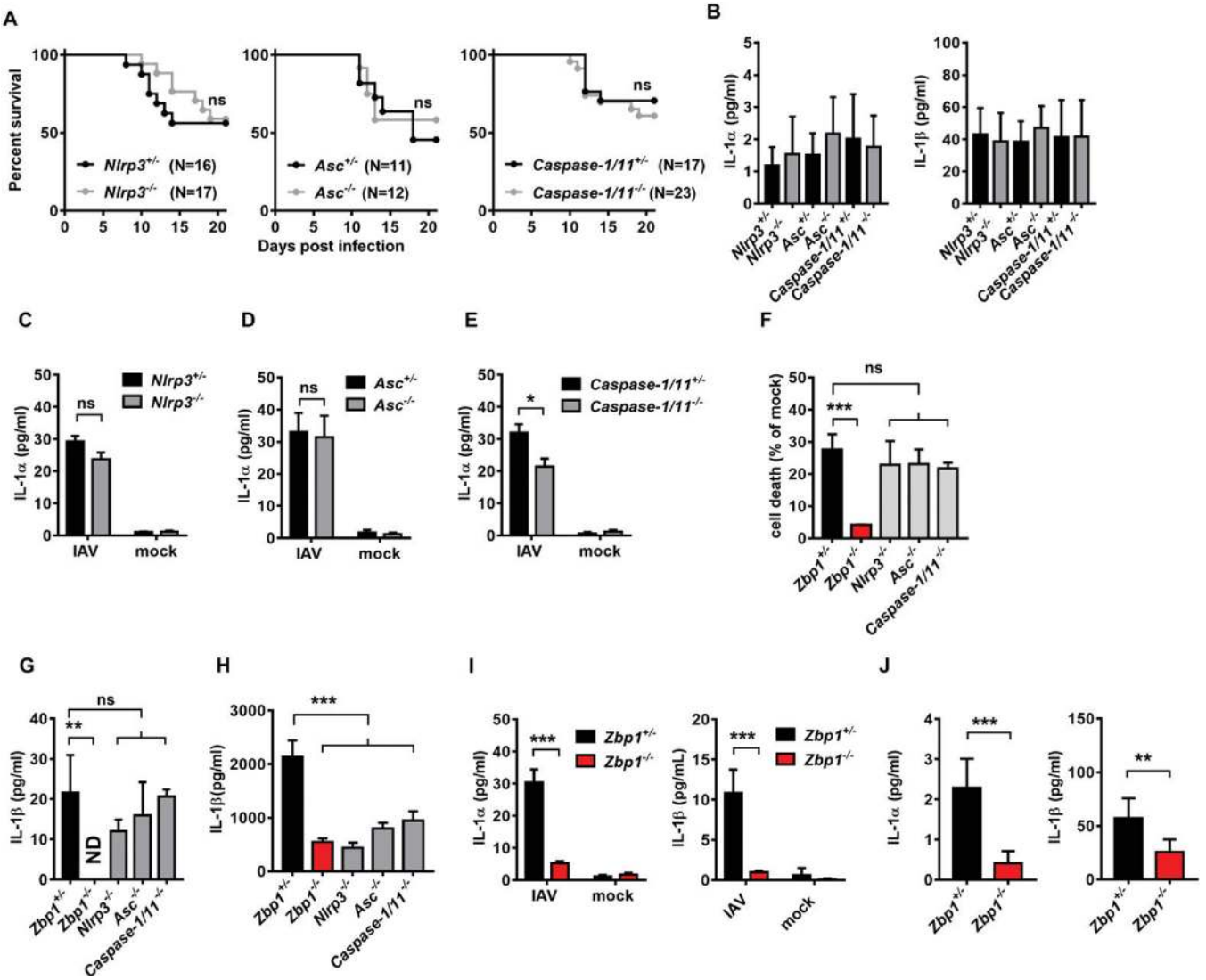

Fig. 2. ZBP1 is essential for inflammasome-independent IL-1 induced by IAV infection. *Nlrp3*$^{+/-}$, *Nlrp3*$^{-/-}$, *Asc*$^{+/-}$, *Asc*$^{-/-}$, *Caspase-1/11*$^{+/-}$ and *Caspase-1/11*$^{-/-}$ mice were infected with IAV and their survival curve (A) and BALF IL-1α levels analyzed on day 3 post-infection are shown (B). Data are pooled from two independent experiments (N = 7–11 per group). BMDMs obtained from *Zbp1*$^{+/-}$, *Zbp1*$^{-/-}$, *Nlrp3*$^{+/-}$, *Nlrp3*$^{-/-}$, *Asc*$^{+/-}$, *Asc*$^{-/-}$, *Caspase-1/11*$^{+/-}$ and *Caspase-1/11*$^{-/-}$ mice were either mock-infected or infected with 10 MOI of IAV without (C-G and I) or with LPS priming (H) for 24 h, and the culture supernatants were collected and the concentrations of IL-1α and IL-1β were measured. BALF IL-1α and IL-1β secretion levels of *Zbp1*$^{+/-}$ and *Zbp1*$^{-/-}$ (N = 5 per group) were determined by ELISA on day 3 after IAV infection (J). Statistical significances between each survival curve for the mice were determined by log-rank (Mantel–Cox) test (A). Error bars represent mean ± SD of technical triplicate. NS, not significant. *P < 0.05, **P < 0.005, ***P < 0.001. Similar ELISA results were obtained from at least two separate experiments.

(Fig. 2J) were shown to produce significantly lower IL-1α compared to the control group, although IAV infection induces ZBP1-dependent cell death in both alveolar macrophages and lung fibroblasts (Supplementary Figure S1B), lung fibroblasts did not release the IL-1α after IAV infection (Supplementary Figure S1C), suggesting the pivotal role of ZBP1 in both cell death and IL-1α secretion, while the NLRP3 inflammasome was not necessary in our experimental setting for both cell death (Fig. 2F) and IL-1α secretion *in vitro* and *in vivo* (Fig. 2B–E, I and J). It is of note that the prior treatment with LPS with IAV infection exhibited both ZBP1 and NLRP3 inflammasome-dependent IL-1β secretion (Fig. 2H). Thus, these data above clearly show that not only IL-1β, but also IL-1α is induced and secreted during IAV infection, which coincides with ZBP1-dependent cell death and plays a critical role inNLRP3 inflammasome-independent, IL-1-mediated immune activation.

The hierarchical relationship between ZBP1-dependent cell death and NLRP3 inflammasome activation is still elusive, but it is conceivable that ZBP1-mediated, but inflammasome-independent cell death and the initial IL-1α secretion trigger the positive feedback through IL-1R, leading to the optimal IL-1β induction/secretion (Figs 1 and 2). In support of this idea, we observed that alveolar macrophages in BALF were diminished after IAV infection, although *ZBP1*$^{-/-}$ mice had more alveolar macrophages (data not shown). On the other hand,

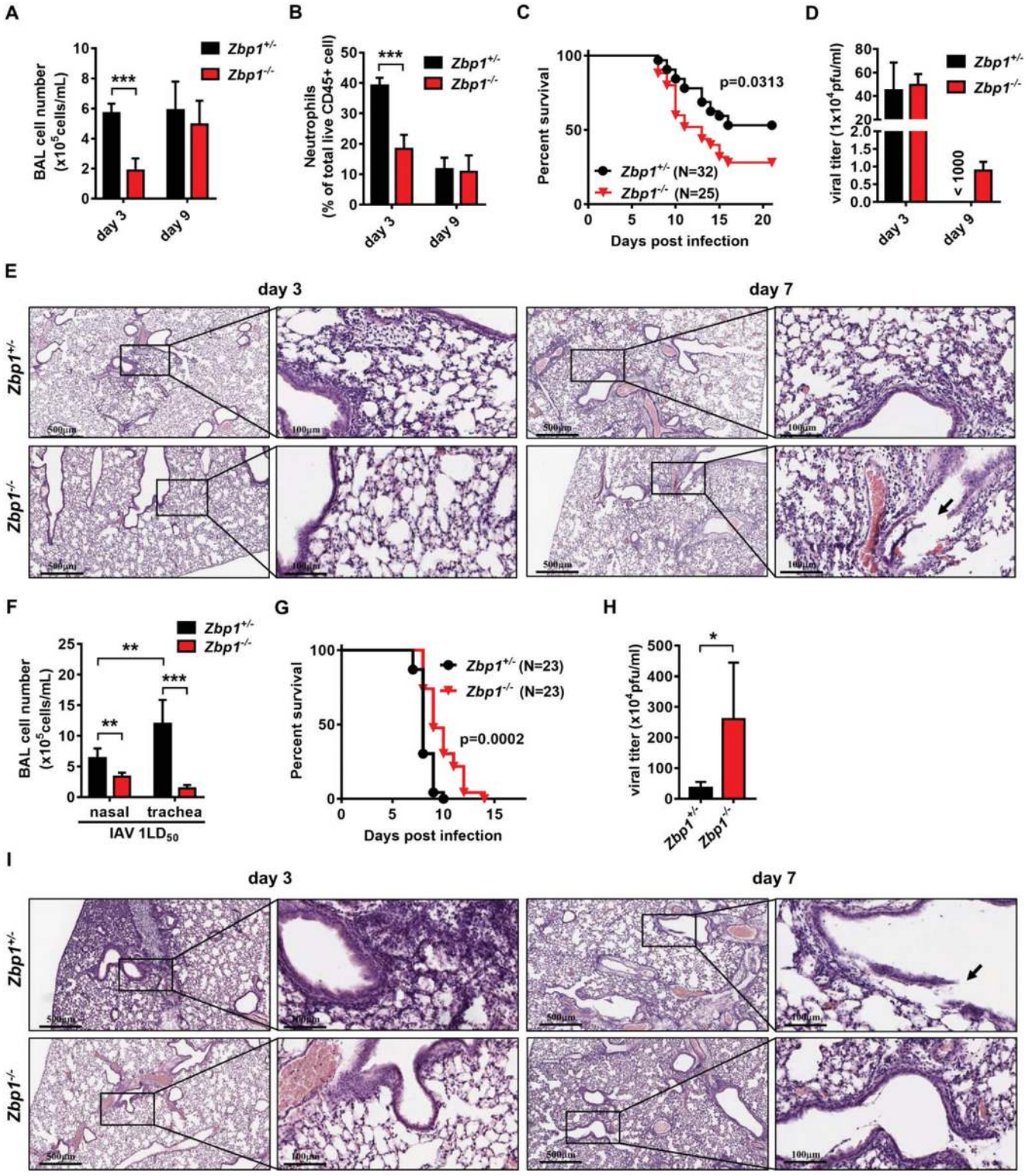

Fig. 3. ZBP1 controls IAV-induced acute lung inflammation and viremia, but the resultant pathogenesis depends on the mode (route) of infection. *Zbp1*$^{+/-}$ and *Zbp1*$^{-/-}$ mice were infected with IAV intra-nasally (A–E) or intra-tracheally (F–I). Mice were sacrificed at various time point after infection as indicated, and the total number of live CD45-positive cells (A, F), its neutrophil percentages (B), their survival rate (C, G), the lung viral titer (D, H) and histological analysis of the infected, H&E-stained lung (E, I) were analyzed and shown as indicated. BALF IAV titer (D, H) was determined by standard plaque assay in MDCK cells on day 3 for both routes of infection and day 9 for intra-nasal infection ($N = 5$ per group). Representative lung H&E staining images (E, I) of *Zbp1*$^{+/-}$ and *Zbp1*$^{-/-}$ mice on day 3 or 7 ($N = 4$–6) are shown and the arrows on day 7 images indicate the exfoliation of bronchiolar epithelial cells as severe pulmonary damage. BALF (A, B, F) were collected on day 3 after intra-nasal or intra-tracheal IAV infection ($N = 8$ per group). Statistical significances between each mice survival curve were determined by log-rank (Mantel–Cox) test (C and G). Error bars represent mean ± SD. *$P < 0.05$, **$P < 0.005$, ***$P < 0.001$. Similar ELISA, IAV titer, H&E staining and BAL cell number results were obtained from at least two separate experiments.

it is likely that more robust NLPR3-inflammasome-dependent production of IL-1β can take place when the host is infected with high-dose IAV, in which the direct and viral RNA-mediated innate immune activation of immune cells, rather than indirect events, occur only during or after viral replication (Supplementary Figure S1D), or other immunological insults like LPS priming that increase the expression of not only the transcript of IL-1α, but also IL-1β and NLRP3 via NF-kB-dependent signaling pathways (38), licensing the NLRP3-inflammasome-mediated IL-1β production. Nevertheless, our results above added ZBP1-mediated IL-1α as one of the inflammatory feedback loops during the acute stage of IAV infection (4, 32)

Physiological roles of ZBP1-dependent cell death and IL-1α in the host defense against IAV infection

IAV infection often induces severe pulmonary inflammation which is the determining factor in its morbidity and mortality (39). There are two studies that investigated the role of ZBP1 in IAV infections, and they both demonstrated the indispensable role of ZBP1 in IAV-induced cell death and IL-1-mediated inflammatory responses *in vitro* and *in vivo*; however, its physiological relevance to IAV infection is controversial. One group reported that ZBP conferred protective immunity (20), where the other group suggested ZBP1 contributed to pathogenesis caused by acute IAV infection (22). To elucidate the controversy and examine the physiological role of ZBP1-dependent cell death and IL-1α secretion in IAV infection in our experimental settings, we infected *Zbp1*$^{+/-}$ and *Zbp1*$^{-/-}$ mice either intra-nasally or intra-tracheally with $1LD_{50}$ of IAV.

In intra-nasal infection, *Zbp1*$^{-/-}$ mice, compared with the control *Zbp1*$^{+/-}$, displayed significantly lower numbers of BALF cells (Fig. 3A) as well as neutrophils (Fig. 3B) on day 3, but not day 7 after IAV infection (Fig. 3E), resulting in the reduced survival at 20 days after the infection (Fig. 3C), likely due to delayed virus clearance (Fig. 3D) and increased pulmonary damage in later phases of infection (Fig. 3E).

We then infected *Zbp1*$^{+/-}$ and *Zbp1*$^{-/-}$ mice with IAV via the intra-tracheal route, which is thought to enhance acute phase pulmonary damage (40, 41). Indeed, intra-tracheal challenge induced higher pulmonary inflammation based on BALF cell number (Fig. 3F) and a shortened survival time (Fig. 3G) compared to an equal dose of intra-nasal challenge. In stark contrast to intra-nasal challenge, intra-tracheally challenged *Zbp1*$^{-/-}$ mice showed significantly lower mortality than *Zbp1*$^{+/-}$ mice (Fig. 3G), although mice still showed delayed viral clearance on day 7 (Fig. 3H). As with intra-nasal challenge, *Zbp1*$^{-/-}$ mice showed lower pulmonary damage during the acute phase (Fig. 3I).

It is of noteworthy that the data obtained by intra-tracheal infection of *Zbp1*$^{-/-}$ mice were consistent with results shown by Kuriakose *et al.* (22), while the data obtained by intra-nasal infection of *Zbp1*$^{-/-}$ mice were in line with Thapa *et al.* (20). It is well known that different doses and strains of IAV lead to diverse inflammatory responses and immunopathology in the lung, which is highly correlated with host mortality (2, 4). For example, RIP3 deficiency causes increased mortality to the A/Puerto Rico/8/34 (PR8) strain of IAV (19), but decreased mortality to the highly pathogenic H7N9 strain (42). Taken together, our data suggest that ZBP1-dependent cell death controls IL-1α secretion, which can have either a beneficial or detrimental role that depends on either upper (mild) or lower (severe) airway infection with IAV, respectively, which may explain the current controversy related to the physiological role of ZBP1 in pathogenesis (22) or protection (20) during IAV infection.

ZBP1 controls neutrophil influx and NET formation into the lung after IAV infection

IL-1α and IL-1β are potent initiators for neutrophil influx and infiltration to the lung, which had been reported as both beneficial (43, 44) and detrimental (4, 45) factors for host protection against IAV infection. We therefore examined whether ZBP1 deficiency has effects on, and plays a role in, the neutrophil influx and infiltration into the lung, when the mice were infected with IAV. *Zbp1*$^{+/-}$ and *Zbp1*$^{-/-}$ mice were infected with IAV intra-nasally, and the lung tissue was applied to 2-photon microscopic 3D imaging analysis as well as the BALF cells being analyzed by using image flow cytometry. In the IAV-infected lung and BALF, neutrophil influx and infiltration were observed, all of which were significantly reduced in *Zbp1*$^{-/-}$ mice compared with *Zbp1*$^{+/-}$ (Figs. 3B and 4A). In particular, we found both under the 2-photon microscopy and image flow cytometry, abundant examples of NETs in the infected lung sections and BALF, respectively (Fig. 4A). As indicated (Fig. 4C and D), DNA-positive, string-like structures were observed in the infected lung peripheral tissue, and were significantly reduced in the infected *Zbp1*$^{-/-}$ mice (Fig. 4A and B and Supplementary Movie 1 and 2). Consistent with these observations, infected *Zbp1*$^{-/-}$ mice showed lower double-stranded DNA (dsDNA) levels in BALF compared to *Zbp1*$^{+/-}$ mice (Fig. 4C). To confirm and quantify the presence of NETs, rather than just dsDNA released from dying cells, we performed imaging flow cytometry of BALF cells from infected mice using a method we recently developed (26). NETs in BALF were readily identified based on the presence of Ly6G-positive cells with DNA-positive extracellular structures (Fig. 4A and B; Supplementary Figure S3), and quantification based on this method indicated a significant reduction of NETs in *Zbp1*$^{-/-}$ mice (Fig. 4B and D; Supplementary Figure S3B). NETs have been shown to directly cause epithelial and endothelial cell death, and thereby it is plausible that they would contribute to acute lung pathology (45, 46). Finally, to further investigate the physiological role of neutrophils and NETs in IAV infection, we depleted neutrophils via injection of anti-Ly6G antibody. In wild-type mice, neutrophil depletion reduced survival (Fig. 4G), supporting a role of neutrophils in controlling IAV infection (43). In this setting, no differences in acute lung damage or survival were observed in neutropenic *Zbp1*$^{+/-}$ and *Zbp1*$^{-/-}$ mice (data not shown). Moreover, neutrophil depletion extended the survival time and protected the *Zbp1*$^{+/-}$ mice from intra-tracheal IAV infection, in spite of a lower effect on the survival of *Zbp1*$^{-/-}$ mice (data now shown), suggesting that neutrophils play an essential role in the observed phenotype of ZBP1 deficient mice. Furthermore, while IL-1β secretion was dependent on neutrophils (Fig. 4F), IL-1α secretion was unaffected (Fig. 4E), suggesting a key

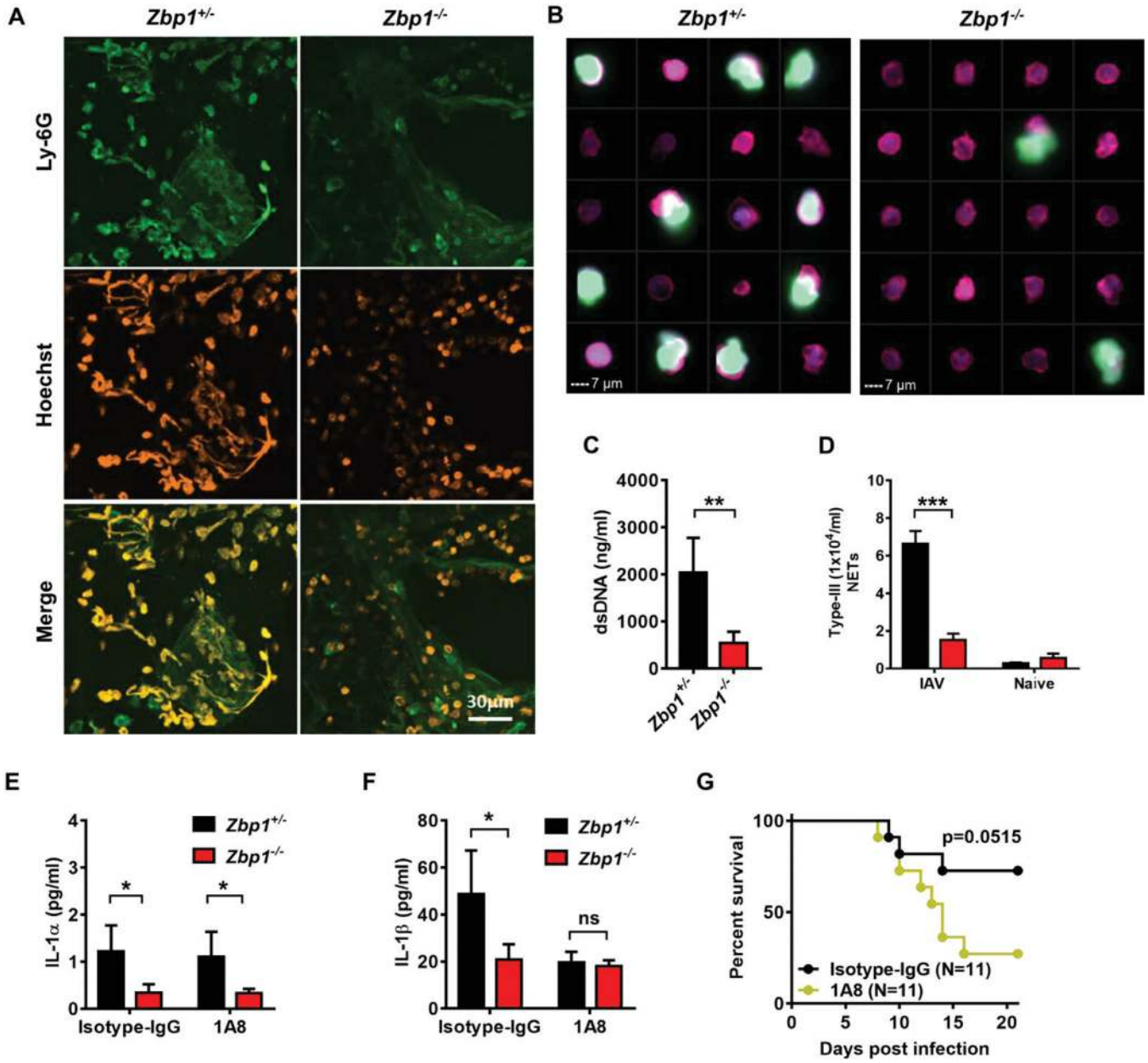

Fig. 4. ZBP1 is required for the optimal lung neutrophil infiltration, DNA release and NET formation after IAV infection. *Zbp1*$^{+/-}$ or *Zbp1*$^{-/-}$ mice were infected intra-nasally with IAV. At day 3 after IAV infection, neutrophils and DNA in the infected lung were stained by FITC-anti-Ly6G antibody and Hoechst 33342 analyzed by a 2-photon microscope (A). Quantitated and qualitative analysis of BALF neutrophils and type III NETs (Supplementary Figure S3) (26) from IAV-infected *Zbp1*$^{+/-}$ and *Zbp1*$^{-/-}$ mice were obtained by imaging flow cytometry, as stained with PE-Cy7-conjugated anti-Ly6G antibody (pink) and DNA by SytoxGreen; SYG (green) and Hoechst; HO (purple) (B, D). In addition, the concentrations of DNA in the same BALF were measured (C). BALF IL-1α (E) and IL-1β (F) secretion levels from neutrophil-depleted *ZBP1*$^{+/-}$ and *ZBP1*$^{-/-}$ mice on day 3 after IAV infection. Survival analysis of neutrophil-depleted wild-type mice infected with IAV intra-nasally (G). Statistical significances between each survival curve for the mice were determined by log-rank (Mantel–Cox) test (G). All data are representative from two independent experiments. Error bars represent mean ± SD. $^{*}P < 0.05$, $^{**}P < 0.005$, $^{***}P < 0.001$.

role of neutrophils in IL-1β induction acting downstream of ZBP1-meditated IL-1α (Figs 1 and 2). This idea is supported by previous studies which demonstrate that hematopoietic cells such as alveolar macrophages and neutrophils can act as source of IL-1β in the alveolar space (7), and in concert to create an inflammatory feedback loop (4). A recent study showed that IL-1β can be activated by neutrophil-derived mCRAMP, potentially enhancing this inflammatory response (32). Therefore, ZBP1-mediated IL-1α in the acute lung pathology caused by IAV may well explain its reciprocal roles in the neutrophil response to IAV, resulting in either protective or pathological outcomes (20, 22).

Previous reports in IL-1R-deficient mice also showed delayed viral clearance, which was attributed to reduced CD4^{+}

cell-dependent immunoglobulin responses (6) or reduced CD8+ cell-dependent cellular immunological responses (29) on day 7 and day 9 or 14 time points, respectively. A recent study also showed that IL-1α administration during the early phase of IAV infection induces germinal center maturation and iBALT formation (47) which is responsible for priming of influenza specific B- and T-cell proliferation and responses (48). Consistent with these reports, we found reduced IgM induction but normal levels of CD8+ anti-NP tetramer numbers on day 7 after IAV infection (Supplementary Figure S2A and B), indicating that ZBP1-dependent IL-1 induction is important for the development of acquired immunity and viral clearance in later stages of IAV infection. In particular, the importance of IgM induced by initial IAV infection may well be accounted as the critical role of IgM in protective immune response to IAV infection as indicated by previous works (49–52).

Overall, our study outlines a model in which ZBP1-dependent cell death, IL-1α induction, and neutrophil infiltration and NET formation are key pathological and immune factors which ultimately dictate survival during IAV infection. We propose that initial ZBP1-dependent cell death induced by IAV infection leads to IL-1α induction and release in the lung. IL-1α then plays a key role in IL-1β induction and together these cytokines promote infiltration of inflammatory neutrophils to the lung. Infiltrating neutrophils go on to form NETs which may result in either outcome after IAV infection, both of which nevertheless cause pathological damage to lung tissue. Our findings also highlight the importance of an IL-1α-initiated inflammatory feedback loop, which has been reported in other virus infections (53) and during sterile inflammation (31), but has been overlooked in IAV infection. Our results suggest that the balance of these factors can lead to both increased pathology and death during severe infection, but also to improved acquired immunity and survival in milder infection. Our results shed light on the importance of ZBP1 and IL-1α as master controllers of neutrophil dependent pulmonary inflammation in IAV infection, and reveal them as potential therapeutic targets to limit excessive IAV-induced acute pulmonary damage.

Funding

This work was supported by National Institutes of Biomedical Innovation, Health and Nutrition, and grants from Japan Science and Technology Agency (JST) CREST(grant number JPMJCR18H1), PRESTO (JPMJPR17H4) and Japan Agency for Medical Research and Development (AMED) (grant numbers are JP17ak0101068, JP18ak0101068 and 17fm0208021h0001). P.L. is a JSPS International Fellow.

Acknowledgements

We wish to acknowledge generous support and suggestions from Prof. Yoshihiro Kawaoka (IMS, University of Tokyo), Dr Jun Kunisawa (NIBIOHN), Dr Norifumi Iijima (NIBIOHN), Prof. Tomohiro Kurosaki (IFREC, Osaka University), Prof. Toshihiro Horii (RIMD, Osaka University), Prof. Atsushi Kumanogoh (School of Medicine, Osaka University) and technical/logistical support from Akiko Okabe and Mayu Kamada (NIBIOHN). K.J.I., C.C., E.K., Y.I. and K.K. designed research and oversaw the project related to the manuscript. K.J.I. and S.A. generated ZBP1 KO mice. M.M. performed most of the infection studies *in vivo* and *in vitro*. M.M., P.L., A.K., T.K. performed analysis of the experiments. M.M., C.C., K.K., E.K. and K.J.I. wrote the manuscript.

Conflicts of interest statement: the authors declared no conflicts of interest.

References

1 Baskin, C. R., Bielefeldt-Ohmann, H., Tumpey, T. M. *et al.* 2009. Early and sustained innate immune response defines pathology and death in nonhuman primates infected by highly pathogenic influenza virus. *Proc. Natl Acad. Sci. USA* 106:3455.
2 Perrone, L. A., Plowden, J. K., García-Sastre, A., Katz, J. M. and Tumpey, T. M. 2008. H5N1 and 1918 pandemic influenza virus infection results in early and excessive infiltration of macrophages and neutrophils in the lungs of mice. *PLoS Pathog.* 4:e1000115.
3 Kash, J. C., Tumpey, T. M., Proll, S. C. *et al.* 2006. Genomic analysis of increased host immune and cell death responses induced by 1918 influenza virus. *Nature* 443:578.
4 Brandes, M., Klauschen, F., Kuchen, S. and Germain, R. N. 2013. A systems analysis identifies a feedforward inflammatory circuit leading to lethal influenza infection. *Cell* 154:197.
5 Teijaro, J. R., Walsh, K. B., Rice, S., Rosen, H. and Oldstone, M. B. 2014. Mapping the innate signaling cascade essential for cytokine storm during influenza virus infection. *Proc. Natl Acad. Sci. USA* 111:3799.
6 Schmitz, N., Kurrer, M., Bachmann, M. F. and Kopf, M. 2005. Interleukin-1 is responsible for acute lung immunopathology but increases survival of respiratory influenza virus infection. *J. Virol.* 79:6441.
7 Ichinohe, T., Lee, H. K., Ogura, Y., Flavell, R. and Iwasaki, A. 2009. Inflammasome recognition of influenza virus is essential for adaptive immune responses. *J. Exp. Med.* 206:79.
8 Thomas, P. G., Dash, P., Aldridge, J. R. Jr *et al.* 2009. The intracellular sensor NLRP3 mediates key innate and healing responses to influenza A virus via the regulation of caspase-1. *Immunity* 30:566.
9 Allen, I. C., Scull, M. A., Moore, C. B. *et al.* 2009. The NLRP3 inflammasome mediates *in vivo* innate immunity to influenza A virus through recognition of viral RNA. *Immunity* 30:556.
10 Rider, P., Carmi, Y., Guttman, O. *et al.* 2011. IL-1α and IL-1β recruit different myeloid cells and promote different stages of sterile inflammation. *J. Immunol.* 187:4835.
11 Luheshi, N. M., Kovács, K. J., Lopez-Castejon, G., Brough, D. and Denes, A. 2011. Interleukin-1α expression precedes IL-1β after ischemic brain injury and is localised to areas of focal neuronal loss and penumbral tissues. *J. Neuroinflammation* 8:186.
12 Barry, K. C., Fontana, M. F., Portman, J. L., Dugan, A. S. and Vance, R. E. 2013. IL-1α signaling initiates the inflammatory response to virulent *Legionella pneumophila in vivo*. *J. Immunol.* 190:6329.
13 Al Moussawi, K. and Kazmierczak, B. I. 2014. Distinct contributions of interleukin-1α (IL-1α) and IL-1β to innate immune recognition of *Pseudomonas aeruginosa* in the lung. *Infect. Immun.* 82:4204.
14 Dinarello, C. A. 2009. Immunological and inflammatory functions of the interleukin-1 family. *Annu. Rev. Immunol.* 27:519.
15 Di Paolo, N. C. and Shayakhmetov, D. M. 2016. Interleukin 1α and the inflammatory process. *Nat. Immunol.* 17:906.
16 Chen, C. J., Kono, H., Golenbock, D., Reed, G., Akira, S. and Rock, K. L. 2007. Identification of a key pathway required for the sterile inflammatory response triggered by dying cells. *Nat. Med.* 13:851.
17 Eigenbrod, T., Park, J. H., Harder, J., Iwakura, Y. and Núñez, G. 2008. Cutting edge: critical role for mesothelial cells in necrosis-induced inflammation through the recognition of IL-1 alpha released from dying cells. *J. Immunol.* 181:8194.
18 Meng, L., Jin, W. and Wang, X. 2015. RIP3-mediated necrotic cell death accelerates systematic inflammation and mortality. *Proc. Natl Acad. Sci. USA* 112:11007.
19 Nogusa, S., Thapa, R. J., Dillon, C. P. *et al.* 2016. RIPK3 activates parallel pathways of MLKL-driven necroptosis and

FADD-mediated apoptosis to protect against influenza A virus. *Cell Host Microbe* 20:13.
20 Thapa, R. J., Ingram, J. P., Ragan, K. B. *et al.* 2016. DAI senses influenza A virus genomic RNA and activates RIPK3-dependent cell death. *Cell Host Microbe* 20:674.
21 Kesavardhana, S., Kuriakose, T., Guy, C. S. *et al.* 2017. ZBP1/DAI ubiquitination and sensing of influenza vRNPs activate programmed cell death. *J. Exp. Med.* 214:2217.
22 Kuriakose, T., Man, S. M., Malireddi, R. S. *et al.* 2016. ZBP1/DAI is an innate sensor of influenza virus triggering the NLRP3 inflammasome and programmed cell death pathways. *Science Immunology* 1:aag2045.
23 Kuroda, E., Ozasa, K., Temizoz, B. *et al.* 2016. Inhaled fine particles induce alveolar macrophage death and interleukin-1α release to promote inducible bronchus-associated lymphoid tissue formation. *Immunity* 45:1299.
24 Koyama, S., Aoshi, T., Tanimoto, T. *et al.* 2010. Plasmacytoid dendritic cells delineate immunogenicity of influenza vaccine subtypes. *Sci. Transl. Med.* 2:25ra24.
25 Kusakabe, T., Ozasa, K., Kobari, S. *et al.* 2016. Intranasal hydroxypropyl-β-cyclodextrin-adjuvanted influenza vaccine protects against sub-heterologous virus infection. *Vaccine* 34:3191.
26 Lelliott, P. M., Momota, M., Lee, M. S. J. *et al.* 2019. Rapid quantification of NETs *in vitro* and in whole blood samples by imaging flow cytometry. *Cytometry A* 95:565.
27 Kozak, W., Zheng, H., Conn, C. A., Soszynski, D., van der Ploeg, L. H. and Kluger, M. J. 1995. Thermal and behavioral effects of lipopolysaccharide and influenza in interleukin-1 beta-deficient mice. *Am. J. Physiol.* 269(5 Pt 2):R969.
28 Swiergiel, A. H., Smagin, G. N., Johnson, L. J. and Dunn, A. J. 1997. The role of cytokines in the behavioral responses to endotoxin and influenza virus infection in mice: effects of acute and chronic administration of the interleukin-1-receptor antagonist (IL-1ra). *Brain Res.* 776:96.
29 Pang, I. K., Ichinohe, T. and Iwasaki, A. 2013. IL-1R signaling in dendritic cells replaces pattern-recognition receptors in promoting CD8$^+$ T cell responses to influenza A virus. *Nat. Immunol.* 14:246.
30 Dinarello, C. A., Ikejima, T., Warner, S. J. *et al.* 1987. Interleukin 1 induces interleukin 1. I. Induction of circulating interleukin 1 in rabbits *in vivo* and in human mononuclear cells *in vitro*. *J. Immunol.* 139:1902.
31 Rabolli, V., Badissi, A. A., Devosse, R. *et al.* 2014. The alarmin IL-1α is a master cytokine in acute lung inflammation induced by silica micro- and nanoparticles. *Part. Fibre Toxicol.* 11:69.
32 Peiró, T., Patel, D. F., Akthar, S. *et al.* 2018. Neutrophils drive alveolar macrophage IL-1β release during respiratory viral infection. *Thorax* 73:546.
33 Ichinohe, T., Pang, I. K. and Iwasaki, A. 2010. Influenza virus activates inflammasomes via its intracellular M2 ion channel. *Nat. Immunol.* 11:404.
34 Pang, I. K. and Iwasaki, A. 2011. Inflammasomes as mediators of immunity against influenza virus. *Trends Immunol.* 32:34.
35 Rodrigue-Gervais, I. G., Labbé, K., Dagenais, M. *et al.* 2014. Cellular inhibitor of apoptosis protein cIAP2 protects against pulmonary tissue necrosis during influenza virus infection to promote host survival. *Cell Host & Microbe* 15:23.
36 Malik, A. and Kanneganti, T. D. 2018. Function and regulation of IL-1α in inflammatory diseases and cancer. *Immunol. Rev.* 281:124.
37 Ishii, K. J., Kawagoe, T., Koyama, S. *et al.* 2008. TANK-binding kinase-1 delineates innate and adaptive immune responses to DNA vaccines. *Nature* 451:725.
38 Bauernfeind, F. G., Horvath, G., Stutz, A. *et al.* 2009. Cutting edge: NF-kappaB activating pattern recognition and cytokine receptors license NLRP3 inflammasome activation by regulating NLRP3 expression. *J. Immunol.* 183:787.
39 Taubenberger, J. K. and Morens, D. M. 2008. The pathology of influenza virus infections. *Annu. Rev. Pathol.* 3:499.
40 Morales-Nebreda, L., Chi, M., Lecuona, E. *et al.* 2014. Intratracheal administration of influenza virus is superior to intranasal administration as a model of acute lung injury. *J. Virol. Methods* 209:116.
41 Morita, M., Kuba, K., Ichikawa, A. *et al.* 2013. The lipid mediator protectin D1 inhibits influenza virus replication and improves severe influenza. *Cell* 153:112.
42 Xu, Y. L., Tang, H. L., Peng, H. R., Zhao, P., Qi, Z. T. and Wang, W. 2017. RIP3 deficiency ameliorates inflammatory response in mice infected with influenza H7N9 virus infection. *Oncotarget* 8:27715.
43 Tate, M. D., Deng, Y. M., Jones, J. E., Anderson, G. P., Brooks, A. G. and Reading, P. C. 2009. Neutrophils ameliorate lung injury and the development of severe disease during influenza infection. *J. Immunol.* 183:7441.
44 Tate, M. D., Ioannidis, L. J., Croker, B., Brown, L. E., Brooks, A. G. and Reading, P. C. 2011. The role of neutrophils during mild and severe influenza virus infections of mice. *PLoS ONE* 6:e17618.
45 Narasaraju, T., Yang, E., Samy, R. P. *et al.* 2011. Excessive neutrophils and neutrophil extracellular traps contribute to acute lung injury of influenza pneumonitis. *Am. J. Pathol.* 179:199.
46 Saffarzadeh, M., Juenemann, C., Queisser, M. A. *et al.* 2012. Neutrophil extracellular traps directly induce epithelial and endothelial cell death: a predominant role of histones. *PLoS ONE* 7:e32366.
47 Neyt, K., GeurtsvanKessel, C. H., Deswarte, K., Hammad, H. and Lambrecht, B. N. 2016. Early IL-1 signaling promotes iBALT induction after influenza virus infection. *Front. Immunol.* 7:312.
48 Moyron-Quiroz, J. E., Rangel-Moreno, J., Kusser, K. *et al.* 2004. Role of inducible bronchus associated lymphoid tissue (iBALT) in respiratory immunity. *Nat. Med.* 10:927.
49 Baumgarth, N., Herman, O. C., Jager, G. C., Brown, L. E., Herzenberg, L. A. and Chen, J. 2000. B-1 and B-2 cell-derived immunoglobulin M antibodies are nonredundant components of the protective response to influenza virus infection. *J. Exp. Med.* 192:271.
50 Kopf, M., Brombacher, F. and Bachmann, M. F. 2002. Role of IgM antibodies versus B cells in influenza virus-specific immunity. *Eur. J. Immunol.* 32:2229.
51 Taylor, H. P. and Dimmock, N. J. 1985. Mechanisms of neutralization of influenza virus by IgM. *J. Gen. Virol.* 66 (Pt 4):903.
52 Panda, S. and Ding, J. L. 2015. Natural antibodies bridge innate and adaptive immunity. *J. Immunol.* 194:13.
53 Di Paolo, N. C., Baldwin, L. K., Irons, E. E., Papayannopoulou, T., Tomlinson, S. and Shayakhmetov, D. M. 2014. IL-1α and complement cooperate in triggering local neutrophilic inflammation in response to adenovirus and eliminating virus-containing cells. *PLoS Pathog.* 10:e1004035.